Abstract

Robust Control Design for Yaw Stability of Commercial Vehicles

Dongwoo Park
Mechanical and Aerospace Engineering
The Graduate School
Seoul National University

This paper describes yaw stability control of commercial vehicles. When it comes to commercial vehicles, their unique characteristics – center of gravity, trackwidth, weight distribution – make them particularly vulnerable to yaw instability. In the case of commercial vehicles, variations of vehicle parameters are relatively large compared to passenger vehicles due to their loading conditions. Changes in some parameters, such as mass, cornering stiffness, center of gravity, can result in changes of pole locations. To obtain robust stability control performance, a robust yaw stability controller which takes advantage of stochastic root locus and sensitivity dynamics was used. Simulation studies have been conducted for the evaluation of the proposed controller. It has been

shown via simulations that robust yaw stability control performance robust to parameter variations can be achievable by the use of the controller.

Keywords : Electronic Stability Control, Yaw Stability Control, Commercial Vehicle, Stochastic Root Locus, Sensitivity Dynamics, Linear Quadratic Regulator

Student Number : 2012-20666

Contents

List of Figures

Nomenclatures

m	Vehicle mass
I_x	Vehicle moment of inertia about roll axis
I_y	Vehicle moment of inertia about pitch axis
I_z	Vehicle moment of inertia about yaw axis
l_f	Distance from the center of gravity to the front axle
l_r	Distance from the center of gravity to the rear axle
L	Wheelbase
h	Height of the mass center
t_w	Trackwidth
C_f	Cornering stiffness of a front tire
C_r	Cornering stiffness of a rear tire
γ	Yaw rate
β	Body slip angle
δ_f	Steering wheel angle
F_{x1}	Longitudinal force of front left tire
F_{x2}	Longitudinal force of front right tire
F_{x3}	Longitudinal force of rear left tire
F_{x4}	Longitudinal force of rear right tire
F_{y1}	Lateral force of front left tire
F_{y2}	Lateral force of front right tire
F_{y3}	Lateral force of rear left tire
F_{y4}	Lateral force of rear right tire
F_{z1}	Vertical force of front left tire
F_{z2}	Vertical force of front right tire
F_{z3}	Vertical force of rear left tire

F_{z4}	Vertical force of rear right tire
i	Index of uncertain parameters
0	Initial condition
s	Laplacian operator
v_x	Longitudinal velocity
a_y	Lateral acceleration
R	Radius of a road
u	Control input
pr	Probability
$P(v)$	Plant
$C(d)$	Controller
λ	Eigenvalue(pole)
σ_{th}	Criterion of stability
σ	Real part of a pole
ω	Imaginary part of a pole
μ	Tire-road friction coefficient
ΔF_{x1}	Brake input of front left tire
ΔF_{x2}	Brake input of front right tire
ΔF_{x3}	Brake input of rear left tire
ΔF_{x4}	Brake input of rear right tire

Chapter 1. Introduction

1.1 Research Background

ESC systems use automatic computer-controlled braking of individual wheels to assist the driver in maintaining control in critical driving situations. National Highway Traffic Safety Administration(NHTSA) estimates ESC will reduce single-vehicle crashes of passenger cars by 34% and single vehicle crashes of sport utility vehicles (SUVs) by 59%, with a much greater reduction of rollover crashes. NHTSA estimates ESC would save 5,300 to 9,600 lives and prevent 156,000 to 238,000 injuries in all types of crashes annually once all light vehicles on the road are equipped with ESC [1].

Moreover, ESC is expected to play an important role in reducing accidents of commercial vehicles. In these days, reduction of the number of fatal crashes involving heavy vehicles has been accomplished. Actually, the number of heavy vehicles involved in fatal accidents has been decreased from 4,995 in 2000 to 4,633 in 2007[2]. This improvement states a decrease in the number of crashes involving heavy vehicles per 100 million miles travelled from 2.43 in 2000 to 2007. Despite of such great improvements, further safety advancements are possible. Recently, NHTSA proposed to establish a new Federal Motor Vehicle Safety Standard No. 136 to require electronic stability control (ESC) systems on heavy vehicle tractors and certain buses with a gross vehicle weight rating of greater than 11,793 kilograms (26,000 pounds). In 2012, they expected that about 26 percent of new truck tractors and 80 percent of new buses

affected by this proposed rule would be equipped with ESC systems. Moreover, they estimated that ESC systems could prevent 40 to 56 percent of untripped rollover crashes and 14 percent of loss-of-control crashes[3]. In order to evaluate the effect of commercial vehicle ESC, NHTSA conducted HILS(Hardware-in-the-loop Simulation) test with Meritor WABCO[4].

Various stability control designs for passenger vehicles have been developed. Jnagyeol Yoon and Wanki Cho developed unified chassis control for rollover prevention and lateral stability based on rollover index that uses roll angle – roll rate plane and sliding mode control [5]. Some researches use fuzzy logic which is composed of membership functions of body slip angle, yaw rate to stabilize vehicles [6].

Since commercial vehicles are more likely to be involved in fatal accidents and their impacts are high, suitable stability control strategy is needed for them. There exist various researches about stability control of commercial vehicles. Chen [8] has designed a lateral controller of heavy vehicles by utilizing coordinated steering and braking control algorithm based on multivariable backstepping technique. Tankut Acarman [9] used frequency shaped sliding mode control to prevent rollover of heavy trucks. However, most of them take articulated vehicles into account. Although parameter variation is one of the most representative characteristic of commercial vehicles, control design which deals with this property is not treated in most researches. As outlined by Guvenc [7], a control design for robust yaw stability of commercial vehicles was proposed. The paper is about not yaw moment control but robust steering control and the controller was designed to result in model regulation, disturbance rejection, sensor

noise rejection with respect to uncertain velocity and tire-road friction coefficient. Also, controller design parameters was decided with considering six uncertain cases. However, not only changes in these factors but also variations in some vehicle parameters, such as mass, cornering stiffness, center of gravity can lead to undesired behavior even though a vehicle is controlled. Therefore, considering uncertain vehicle parameters in control is needed. Moreover, uncertain parameters can be addressed well with probabilistic approach.

1.2 Research Overview

In this paper, stochastic robust LQR which takes advantage of stochastic root locus was used to deal with uncertain parameters. Stochastic robustness of linear time-invariant control systems and stochastic root locus are introduced in [10] and [11]. In those papers, probability of exceeding settling time, exceeding control limit, instability were taken into account in order to determine controller parameters. However, in the sense of robustness, considering shape of stochastic root locus is important. Therefore, in this research, several classes of cost function were suggested and minimized in order to guarantee stability, robustness, and small amount of control input.

Sensitivity dynamics was also considered to guarantee robustness of commercial vehicles. Since vehicle parameters can vary, states of the vehicle can be affected by changes of parameters. By considering parameter sensitivity, LQ cost function can be designed differently from conventional LQR[14].

Chapter 2. Vehicle Dynamic Characteristics of Commercial Vehicles

Commercial vehicles are more likely to have uncertain parameters because of their environment – passengers of a bus, freight of a truck. This can be expressed stochastically by setting larger variance of uncertain parameters in case of commercial vehicles than passenger vehicles. In this paper, a bus of 6360 kg was taken to represent a commercial vehicle and a sedan of 1653 kg was used for passenger vehicle. Their nominal vehicle parameters are described in Table. 1.

Table 1. Nominal Vehicle Parameters

	Passenger Vehicle(Sedan)			Commercial Vehicle(Bus)		
	Min	Nominal	Max	Min	Nominal	Max
Mass[kg]	1703	1853	2003	6360	8360	9360
I_x[kg $\cdot m^2$]	614	667.915	721.83	7695.6	8789.4	9883.1
I_y[kg $\cdot m^2$]	2765	2893.6	3022.26	30782.4	37032.4	43282.4
I_z[kg $\cdot m^2$]	2765	2922.5	3080.04	30782.4	37876.4	44969.4
l_f [m]	1.353	1.411	1.469	2.758	3.1275	3.397
l_r [m]	1.579	1.637	1.695	0.9930	1.3625	1.7320
h [m]	0.59	0.605	0.62	1.2	1.25	1.3
t_w [m]	1.6	1.6	1.6	2.030	2.030	2.030
C_f [N/rad]	1.6681×10^4	2.0665×10^4	1.9649×10^4	6.6820×10^4	9.4095×10^4	12.137×10^4
C_r [N/rad]	1.3759×10^4	1.7012×10^4	2.0265×10^4	1.4549×10^5	2.43985×10^5	3.4248×10^5

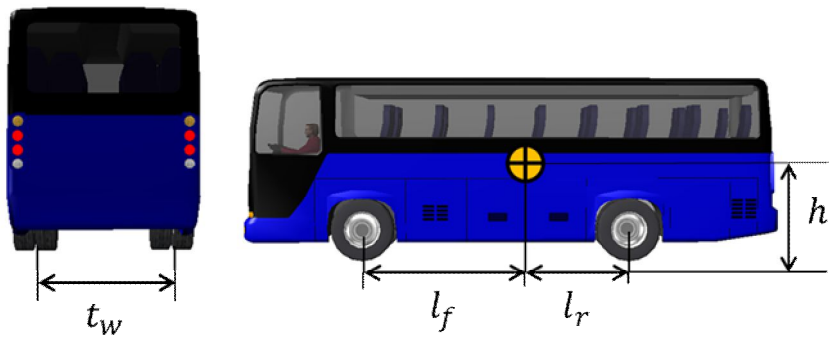

(a) Rear View (b) Side View

Figure 2.1 Vehicle Configuration

By considering capacity of vehicles, calculate maximum value and minimum value of mass variation. Moreover, if we assume that a half of capacity is loaded on the front or rear of the vehicle, maximum l_f or minimum l_f, can be calculated. However, probabilistic distribution of cornering stiffness cannot be easily obtained. Therefore, with various conditions, range of cornering stiffness and its probability density function was analyzed. Firstly, with nominal mass distribution and tire-road friction coefficient, by conducting circle lane tracking and double lane change simulations, cornering stiffness with respect to various lateral acceleration, steering angle, and yaw rate can be obtained as Figure 2.2

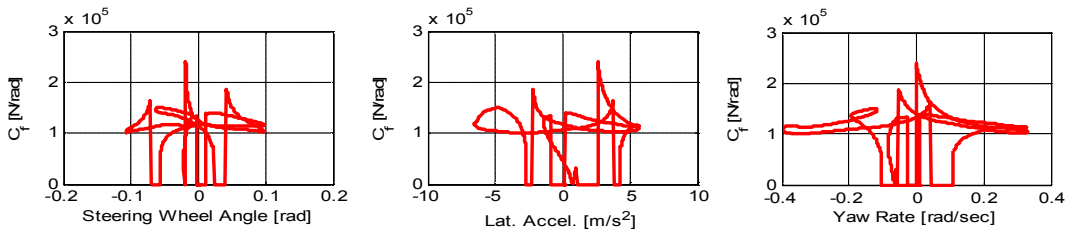

(a) Steering Wheel Angle (b) Lateral Acceleration (c) Yaw Rate

Figure 2.2 Cornering Stiffness

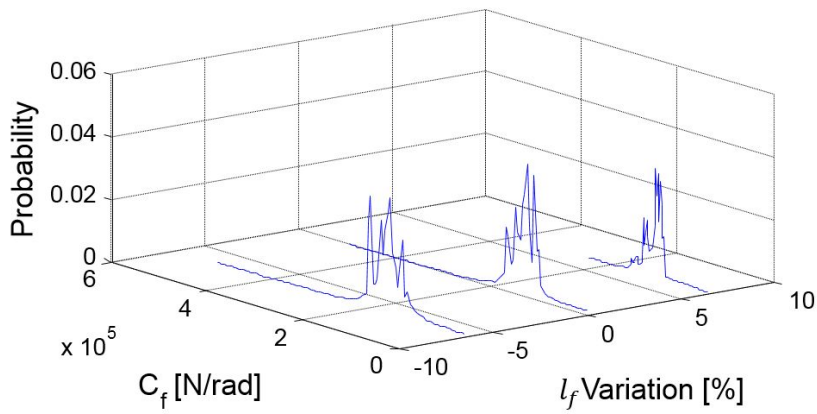

Figure 2.3 Cornering Stiffness PDF with respect to l_f Variation

Likewise, with different l_f, cornering stiffness can be shown as Figure 3. Moreover, multiplication of probability density function of l_f on Figure 2.3 and integrating along l_f was conducted to construct pdf of cornering stiffness considering various maneuvering and mass distribution. Finally, when it comes to tire-road friction

coefficient, cornering stiffness can be assumed to be proportional to the coefficient. Therefore, by assuming that the coefficient has Gaussian distribution with mean of 0.80 and standard deviation of 0.06, identical process of the above can be applied. Probability distributions of uncertain parameters were considered as Gaussian distribution and their standard deviations were assumed to have the value of one-sixth of uncertain ranges. By considering all of the above, overall uncertain ranges of uncertain parameters can be obtained and depicted as Figure 2.4

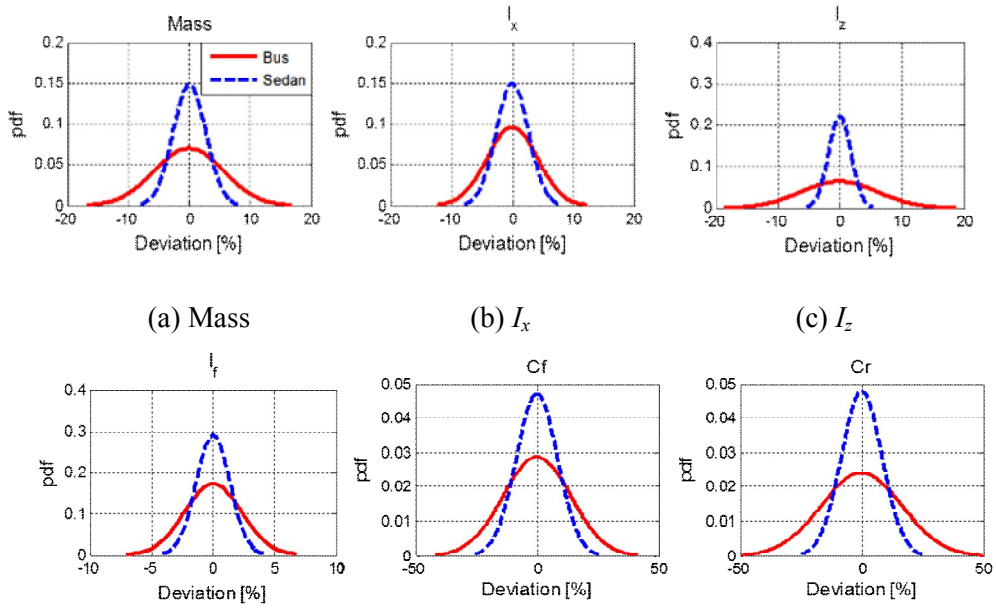

(a) Mass (b) I_x (c) I_z

(d) l_f (e) C_f (f) C_r

Figure 2.4 Probability Density Functions of Uncertain Parameters

2.1 Lateral Dynamics Analysis of Commercial Vehicles

Taking advantage of 3 DOF vehicle planar motion model of Figure 2.5, equations of motions can be obtained as

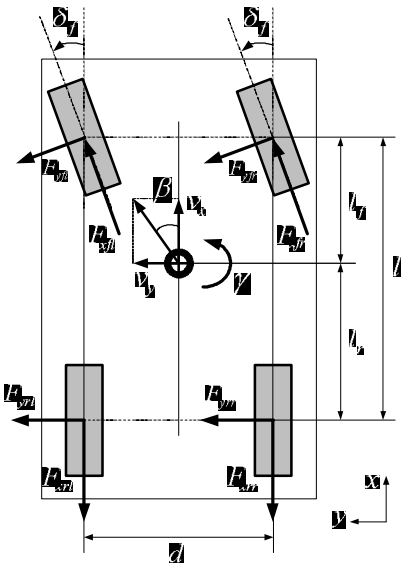

Figure 2.5 3 DOF Vehicle Planar Motion Model

$$
\begin{cases}
m(\dot{v}_x - \gamma v_y) = F_{xr} + F_{xf}\cos\delta_f - F_{yf}\sin\delta_f \\
m(\dot{v}_y + \gamma v_x) = F_{yr} + F_{yf}\cos\delta_f - F_{xf}\sin\delta_f \\
I_z\dot{\gamma} = l_f F_{yf}\cos\delta_f - l_r F_{yr} - l_f F_{xf}\sin\delta_f + \frac{t_w}{2}(\Delta F_{xr} + \Delta F_{xf}\cos\delta_f)
\end{cases}
$$

where,

$$
\begin{aligned}
F_{xf} &= F_{x1} + F_{x2} = F_{xfl} + F_{xfr} \\
F_{yf} &= F_{y1} + F_{y2} = F_{yfl} + F_{yfr} \\
F_{xr} &= F_{x3} + F_{x4} = F_{xrl} + F_{xrr} \\
F_{yr} &= F_{y3} + F_{y4} = F_{yrl} + F_{yrr}
\end{aligned}
\tag{1}
$$

Several assumptions – constant longitudinal speed, sufficiently small body slip angle, identical left and right slip angles – can be developed to simplify the equations. By doing so, equations of motions can be expressed as

$$
\begin{cases}
mv_x\left(\frac{d\beta}{dt} + \gamma\right) = -2C_f\left(\beta + \frac{l_f}{v_x}\gamma - \delta\right) - 2C_r\left(\beta - \frac{l_r}{v_x}\gamma\right) \\
I_z\frac{d\gamma}{dt} = -2C_f\left(\beta + \frac{l_f}{v_x}\gamma - \delta\right)l_f + 2C_r\left(\beta - \frac{l_r}{v_x}\gamma\right)l_r
\end{cases}
\tag{2}
$$

Taking Laplace transformation on (2), the equation becomes as

$$
\begin{cases}
\left\{mv_x s + 2(C_f + C_r)\right\}\beta(s) + \left\{mv_x + \frac{2}{v_x}(l_f C_f - l_r C_r)\right\}\gamma(s) = 2C_f\delta(s) \\
2(l_f C_f - l_r C_r)\beta(s) + \left\{I_z s + \frac{2(l_f^2 C_f + l_r^2 C_r)}{v_x}\right\}\gamma(s) = 2l_f C_f\delta(s)
\end{cases}
\tag{3}
$$

By applying Cramer's rule on (2), yaw rate response and body slip angle response with respect to steering angle can be obtained.

$$\frac{\beta(s)}{\delta(s)} = \frac{\begin{vmatrix} 2C_f & mv_x + \frac{2}{v_x}(l_f C_f - l_r C_r) \\ l_f C_f & I_z s + \frac{2(l_f^2 C_f + l_r^2 C_r)}{v_x} \end{vmatrix}}{\begin{vmatrix} mv_x s + 2(C_f + C_r) & mv_x + \frac{2}{v_x}(l_f C_f - l_r C_r) \\ 2(l_f C_f - l_r C_r) & I_z s + \frac{2(l_f^2 C_f + l_r^2 C_r)}{v_x} \end{vmatrix}} \tag{4}$$

$$\frac{\gamma(s)}{\delta(s)} = \frac{\begin{vmatrix} mv_x s + 2(C_f + C_r) & 2C_f \\ 2(l_f C_f - l_r C_r) & 2l_f C_f \end{vmatrix}}{\begin{vmatrix} mv_x s + 2(C_f + C_r) & mv_x + \frac{2}{v_x}(l_f C_f - l_r C_r) \\ 2(l_f C_f - l_r C_r) & I_z s + \frac{2(l_f^2 C_f + l_r^2 C_r)}{v_x} \end{vmatrix}} \tag{5}$$

Suppose that m ,l_f, C_f, C_r are Gaussian-distributed random variables and their means are their nominal values, standard deviation are values stated above, and vehicle velocity is 70 kph. On top of that, by assuming that all random variables are uncorrelated, root locations will be crowded near their nominal locations. This can be understood by observing Figure 2.6 that describes scatter plot of root locations. In the view of statistics, this scatter plot can be converted to stochastic root locus by applying root density. This can be done by counting the number of roots on subspaces of s-plane with Monte Carlo Evaluation. Stochastic root locus of (4) and (5) are plotted in Figure 2.7

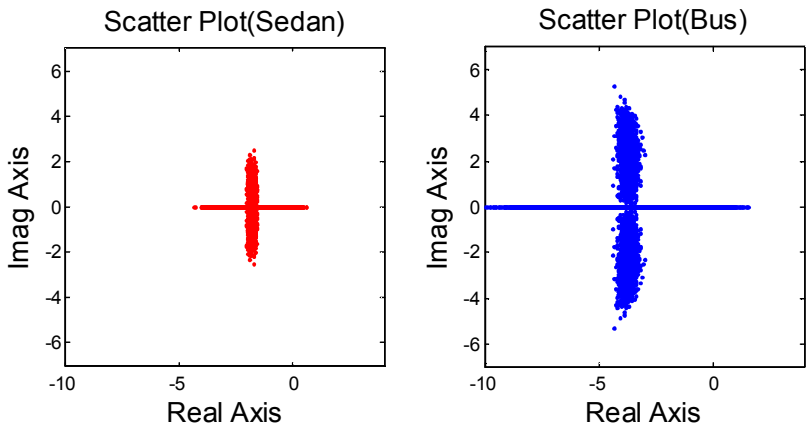

(a) Sedan (b) Bus

Figure 2.6 Scatter Plot of Pole Locations

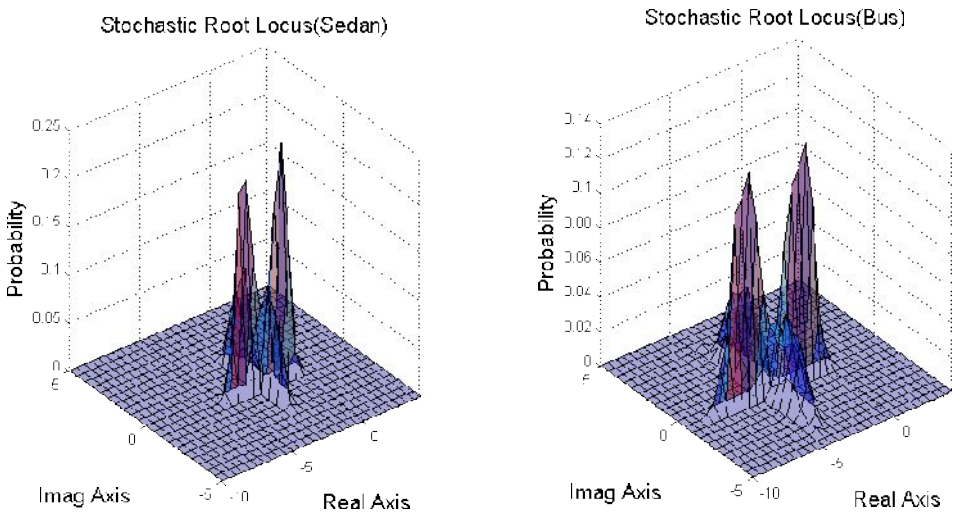

(a) Sedan (b) Bus

Figure 2.7 Stochastic Root Locus

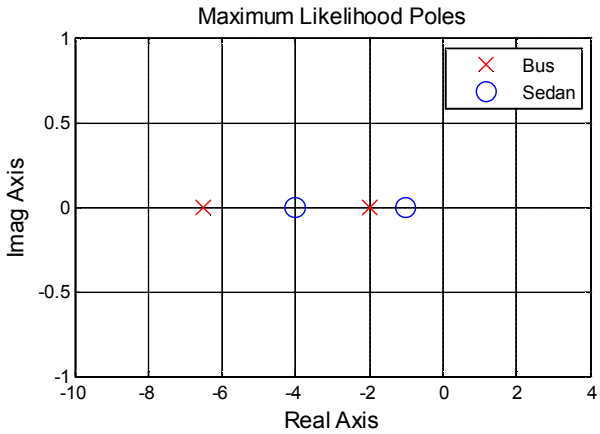

Figure 2.8 Maximum Likelihood Poles

From Figure 2.7, in the case of commercial vehicle, variation of the locus is wider than that of passenger vehicle. Maximum likelihood poles of sedan can be more unstable than those of bus, however, the system can be unstable in the case of bus.

2.2 Sensitivity Dynamics Analysis of Commercial Vehicles

Vehicle states or system matrices can be affected by uncertain parameters. Vehicle parameter dependent model of a commercial vehicle based on (3) can be represented as:

$$\dot{x}(v) = A(v)x + B(v)u$$

$$= \begin{bmatrix} -\dfrac{2(C_f + C_r)}{m \cdot v_x} & -1 - \dfrac{2(l_f \cdot C_f - l_r \cdot C_r)}{m \cdot v_x^{\,2}} \\ -\dfrac{2(l_f \cdot C_f - l_r \cdot C_r)}{I_z} & -\dfrac{2(l_f^{\,2} \cdot C_f + l_r^{\,2} \cdot C_r)}{I_z \cdot v_x} \end{bmatrix} \cdot \begin{bmatrix} \beta \\ \gamma \end{bmatrix}$$

$$+ \begin{bmatrix} \dfrac{2 \cdot C_f}{m v_x} \\ \dfrac{2 \cdot l_f \cdot C_f}{I_z} \end{bmatrix} \cdot \delta_f$$

$$v = \begin{bmatrix} v_1 & v_2 & \cdots & v_p \end{bmatrix} = \begin{bmatrix} C_f, C_r, m, v_x, l_f, l_r, I_z \end{bmatrix} \tag{6}$$

where v is the uncertain vehicle parameter vector.

By differentiating (6), sensitivity vector can be obtained.

$$\dot{\sigma}_i = \bar{A}\sigma_i + \frac{\partial A}{\partial v_i} x + \frac{\partial B}{\partial v_i} u + \bar{B} \frac{\partial u}{\partial v_i}$$

where,

$$\sigma_i = \frac{\partial x}{\partial v_i} \tag{7}$$

Taking advantage of (7), magnitudes of sensitivity vectors can be obtained while a vehicle is running. However, their magnitudes are not suitable to analyze parameter sensitivity since uncertain vehicle parameters' variable ranges are different. Therefore, sensitivity can be analyzed more intuitively and reasonably in the sense of probabilistic way by multiplying respective standard deviation based on Figure 2.4 on each sensitivity vector, and this means

$$\Delta x_i = \left(\frac{\partial x}{\partial v_i} \right) \Delta v_{i,std} \tag{8}$$

To calculate derivative of u with respect to uncertain parameters, u can be expressed as

$$u = \delta_f = \frac{2C_f C_r (l_f + l_r)^2 + m v_x^{\,2} (l_r C_r - l_f C_f)}{2C_f C_r (l_f + l_r) v_x} \gamma \tag{9}$$

Consequently, (7) with respect to each uncertain parameter can be expressed as follows:

$$\dot{\sigma}_m = A\sigma_m + \begin{bmatrix} \frac{2(C_f + C_r)}{m^2 v_x} & \frac{2(C_f l_f - C_r l_r)}{m^2 v_x^{\,2}} \\ 0 & 0 \end{bmatrix} + \begin{bmatrix} \frac{-2C_f}{m^2 v_x} \\ 0 \end{bmatrix} u - B \frac{(C_f l_f - C_r l_r) v_x \gamma}{2C_f C_r (l_f + l_r)}$$

$$\dot{\sigma}_{I_z} = A\sigma_{I_z} + \begin{bmatrix} 0 & 0 \\ \frac{2(C_f l_f - C_r l_r)}{I_z^{\,2}} & \frac{2(C_f l_f^{\,2} + C_r l_r^{\,2})}{I_z^{\,2} v_x} \end{bmatrix} + \begin{bmatrix} 0 \\ \frac{-2C_f l_f}{I_z^{\,2}} \end{bmatrix} u$$

$$\dot{\sigma}_{l_f} = A\sigma_{l_f} + \begin{bmatrix} 0 & \frac{-2C_f}{m v_x^{\,2}} \\ \frac{-2C_f}{I_z} & \frac{-4 l_f C_f}{I_z v_x} \end{bmatrix} + \begin{bmatrix} 0 \\ \frac{2C_f}{I_z} \end{bmatrix} u + B \frac{(2 l_f^{\,2} C_f C_r + 4 l_f C_f C_r l_r - (m(C_f + C_r) v_x^{\,2} - 2C_f C_r l_r) l_r) \gamma}{2(l_f + l_r)^2 C_f C_r v_x}$$

$$\dot{\sigma}_{l_r} = A\sigma_{l_r} + \begin{bmatrix} 0 & \frac{2C_r}{m v_x^{\,2}} \\ \frac{2C_r}{I_z} & \frac{-4 l_r C_r}{I_z v_x} \end{bmatrix} + B \frac{(2 l_r^{\,2} C_f C_r + 4 l_f C_f C_r l_r - (m(C_f + C_r) v_x^{\,2} + 2C_f C_r l_f) l_f) \gamma}{2(l_f + l_r)^2 C_f C_r v_x}$$

$$\dot{\sigma}_{C_f} = A\sigma_{C_f} + \begin{bmatrix} \frac{-2}{m v_x} & \frac{-2 l_f}{m v_x^{\,2}} \\ \frac{-2 l_f}{I_z} & \frac{-2 l_f^{\,2}}{I_z v_x} \end{bmatrix} + \begin{bmatrix} \frac{2}{m v_x} \\ \frac{2 l_f}{I_z} \end{bmatrix} u - B \frac{m l_r v_x \gamma}{4 C_f^{\,2} (l_f + l_r)}$$

$$\dot{\sigma}_{C_r} = A\sigma_{C_f} + \begin{bmatrix} \frac{-2}{m v_x} & \frac{2 l_r}{m v_x^{\,2}} \\ \frac{2 l_r}{I_z} & \frac{-2 l_r^{\,2}}{I_z v_x} \end{bmatrix} + B \frac{m l_f v_x \gamma}{4 C_r^{\,2} (l_f + l_r)}$$

where,

$$\sigma_{i,0} = A^{-1} \left(-\frac{\partial A}{\partial v_i} x_0 - \frac{\partial B}{\partial v_i} u_0 - B \frac{\partial u}{\partial v_i} \right) \tag{10}$$

For instance, during double lane change, sensitivity can be obtained as Figure 2.9.

In most situations, sensitivity with regard to rear cornering stiffness is the largest. Front cornering stiffness sensitivity and I_z sensitivity is also large relative to other parameters.

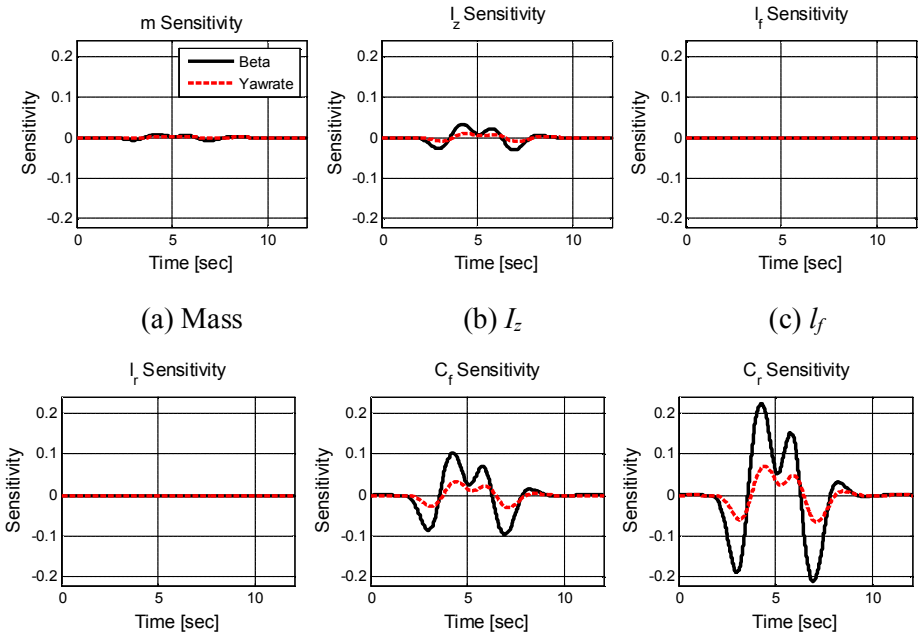

(a) Mass (b) I_z (c) l_f

(d) l_r (e) C_f (f) C_r

Figure 2.9 Sensitivity of uncertain parameters

Chapter 3. Yaw Stability Control of Commercial Vehicles

Comparison between the commercial vehicle and the passenger vehicle provide the fact that the degree of parameter uncertainty is higher for commercial vehicles and the probability of instability is higher in case of commercial vehicles. Therefore, robust control that compensates the uncertainty is needed. First of all, in order to apply LQR, conventional bicycle model is modified. Then design parameters of the controller are determined by considering various cost functions.

3.1 System Model for Stability Analysis

Since steering term exists, even though it is known, stabilization or stability analysis cannot be conducted completely. Therefore, in this paper, steering term was expressed with yaw rate which is the state of the bicycle model. Firstly, by assuming that a vehicle's trajectory is not quite far from its desired track, steering angle can be expressed as[12].

$$\begin{aligned}\delta_f &\approx \frac{l_f + l_r}{R} + \left(\frac{l_r m}{2C_f(l_f + l_r)} - \frac{l_f m}{2C_r(l_f + l_r)} \right) a_y \\ &\approx \frac{l_f + l_r}{R} + \left(\frac{l_r m}{2C_f(l_f + l_r)} - \frac{l_f m}{2C_r(l_f + l_r)} \right) \frac{v_x^{\,2}}{R}\end{aligned} \tag{11}$$

If the vehicle is regarded as behaving circular motion for short time, yaw rate can be represented as follows.

$$\gamma \approx \frac{v_x}{R} \tag{12}$$

Consequently, steering angle can be expressed with yaw rate.

By inserting (11) to (6), at last, modified state equation can be obtained as follows.

$$\dot{x} = \begin{bmatrix} \dot{\beta} \\ \dot{\gamma} \end{bmatrix}$$
$$= \begin{bmatrix} -\frac{2(C_f + C_r)}{m \cdot v_x} & -1 - \frac{2(l_f \cdot C_f - l_r \cdot C_r)}{m \cdot v_x^2} + \frac{4C_f^2 C_r (l_f + l_r)^2 + 2mC_f v_x^2 (l_r C_r - l_f C_f)}{2mC_f C_r (l_f + l_r) v_x^2} \\ -\frac{2(l_f \cdot C_f - l_r \cdot C_r)}{I_z} & -\frac{2(l_f^2 \cdot C_f + l_r^2 \cdot C_r)}{I_z \cdot v_x} + \frac{4l_f C_f^2 C_r (l_f + l_r)^2 + 2l_f C_f m v_x^2 (l_r C_r - l_f C_f)}{2I_z C_f C_r (l_f + l_r) v_x} \end{bmatrix} \cdot \begin{bmatrix} \beta \\ \gamma \end{bmatrix} + \begin{bmatrix} 0 \\ \frac{1}{I_z} \end{bmatrix} \cdot M_z$$
$$= Ax + Bu \tag{13}$$

3.2 Conventional Linear Quadratic Regulator

Conventional Linear Quadratic Regulator(LQR)is introduced in this section. Nominal LQR is the controller that calculates the control input which minimizes following control cost function(J_c).

$$J_c = \int_0^\infty (x^T Q_c x + u^T R_c u) dt$$
$$where, \tag{14}$$
$$Q_c = \begin{bmatrix} q_{1,c} & 0 \\ 0 & q_{2,c} \end{bmatrix}, R_c = r_c$$

Feedback gain can be calculated as

$$K_c = R_c^{-1} B^T P_c$$
$$where, \tag{15}$$
$$A^T P_c + P_c A - P_c B R_c^{-1} B^T P_c + Q_c = 0$$

3.3 Robust Control Design

In this section, robust Linear Quadratic Regulator(LQR) is introduced which reduces parameter sensitivity proposed in section 2.3. Therefore, state feedback control is used. (7) can be represented with u=Kx as

$$\dot{\sigma}_i = (\bar{A}_m - \bar{B}_m K)\sigma_i + (\frac{\partial A_m}{\partial v_i} - \frac{\partial B_m}{\partial v_i} K)x \tag{16}$$

Since first term is stabilized by feedback control, last term should be reduced to guarantee insensitivity toward uncertain parameters. Considering (16), LQ cost function can be expressed as[14]

$$J_r = \int_0^\infty (x^T \begin{bmatrix} Q_r + \rho_{C_r}(\frac{\partial A}{\partial v_{C_r}} - \frac{\partial B}{\partial v_{C_r}} K_r)^T (\frac{\partial A}{\partial v_{C_r}} - \frac{\partial B}{\partial v_{C_r}} K_r) \\ +\rho_i(\frac{\partial A}{\partial v_i} - \frac{\partial B}{\partial v_i} K_r)^T (\frac{\partial A}{\partial v_i} - \frac{\partial B}{\partial v_i} K_r) \end{bmatrix} x + u^T R_r u)dt$$

where,

$$Q_r = \begin{bmatrix} q_{1,r} & 0 \\ 0 & q_{2,r} \end{bmatrix}, R_r = r_r \tag{17}$$

Subscript i means most sensitive parameter based on sensitivity dynamics analysis of section 2.3 except rear cornering stiffness. For arbitrary Q and R matrices, feedback gain can be calculated as

$$K_r = R_r^{-1} B_m^T P_r$$
$$where,$$
$$A_m^T P_r + P_r A_m - P_r B_m R_r^{-1} B_m^T P_r + Q_r$$
$$+\rho_{C_r}\left(\frac{\partial A_m}{\partial v_{C_r}} - \frac{\partial B_m}{\partial v_{C_r}} K_r\right)^T \left(\frac{\partial A_m}{\partial v_{C_r}} - \frac{\partial B_m}{\partial v_{C_r}} K_r\right)$$
$$+\rho_i\left(\frac{\partial A_m}{\partial v_i} - \frac{\partial B_m}{\partial v_i} K_r\right)^T \left(\frac{\partial A_m}{\partial v_i} - \frac{\partial B_m}{\partial v_i} K_r\right) = 0 \tag{18}$$

In order to obtain K through (18), gradient method was used[15]. With calculated K, various cost functions to minimize can be considered and calculated with Monte Carlo Run as

$$P_{A,1} = \int_Q I_1\left[P(v), C(d)\right] pr(q) dq$$
$$where, I_1 = \begin{cases} 1, \text{if } real(\lambda) > \sigma_{th} \\ 0, \text{otherwise} \end{cases} \tag{19}$$

$$P_{B,1} = \int \int I_2\left[pr(\lambda)\right] d\sigma d\omega$$
$$where, I_2 = \begin{cases} 1, \text{if } pr(\lambda) \neq 0 \\ 0, \text{otherwise} \end{cases} \tag{20}$$

$P_{A,1}$ is probability of pole locations' real parts being larger than certain value σ_{th}, and $P_{B,1}$ is projected area on s-plane of stochastic root locus with respect to system model of (13). d of (17) means design parameter vector and for this research, d is (21).

$$d = \left[q_1, q_2, r, \rho_{C_r}, \rho_i\right] \tag{21}$$

Overall cost function is expressed with sum of (19), (20), with weightings.

$$J = w_{A,1} P_{A,1} + w_{B,1} P_{B,1} \tag{22}$$

For various values of design parameters, find suitable values of them to minimize (22) to obtain stability and robustness in the sense of stochastic root locus. Overall control design procedure can be depicted as the flow of Figure 3.1.

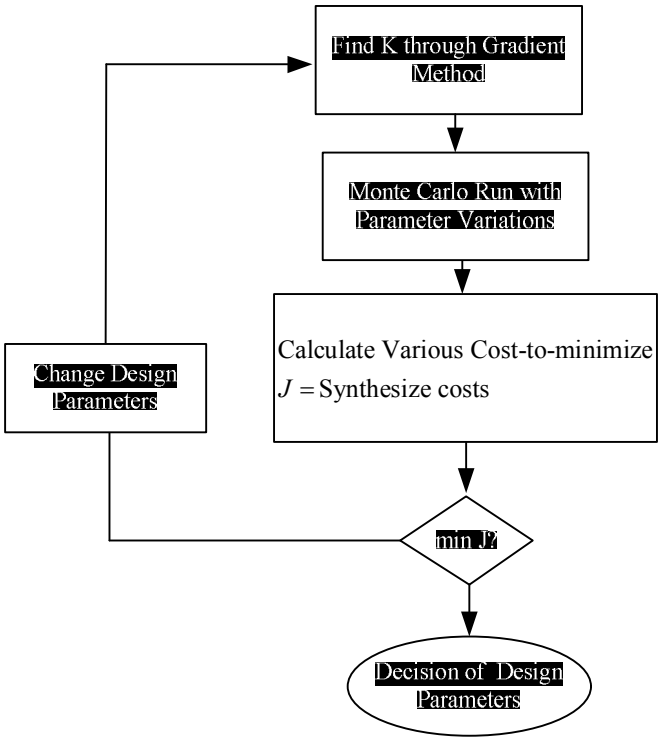

Figure 3.1 Robust Control Design Procedure

$P_{A,1}$ is related to degree of stability directly.$P_{B,1}$ represents 'robustness' since if $P_{B,1}$ is low, system's response is insensitive to parameter uncertainty. Therefore, if a designer want to guarantee high degree of stability, setting $w_{A,1}$ large would be preferred. When robustness is a key objective, large $w_{B,1}$ would be suitable.

In the case of the commercial vehicle of this paper, its understeer coefficient is almost zero which means the vehicle shows almost neutral steer behavior when it is in

cornering circumstance. Therefore, desired yaw rate can be designed as (23) to make vehicle behave neutral steer motion. Moreover, since (23) does not depend on uncertain parameters, in the view of robustness, (23) is suitable for robust control [12].

$$\gamma_{des} = \frac{v_x}{L} \cdot \delta_f \tag{23}$$

Control input can be calculated as follows, at last.

$$u = M_z = -K(x - x_{des})$$

$$where,$$

$$x = \begin{bmatrix} \beta \\ \gamma \end{bmatrix}, x_{des} = \begin{bmatrix} 0 \\ \frac{v_x}{L} \cdot \delta_f \end{bmatrix} \tag{24}$$

3.4 Tire Force Distribution for Yaw Stability Control

When the desired yaw moment is determined, braking force need to be distributed to generate the moment. If the moment is counterclockwise, braking forces are exerted on left tires. In case of clockwise, right tires are used only. Front and rear distribution is conducted by considering the fact that longitudinal acceleration affects tires' friction circles. This can be expressed mathematically by (25).

$$M_{z,des} \geq 0$$

$$\Rightarrow \begin{cases} \Delta F_{x1} = \dfrac{\left|\Delta F_{x1,\max}\right|}{\left|\Delta F_{x1,\max} + \Delta F_{x3,\max}\right|} \Delta F_{x,left} \\ \Delta F_{x3} = \dfrac{\left|\Delta F_{x3,\max}\right|}{\left|\Delta F_{x1,\max} + \Delta F_{x3,\max}\right|} \Delta F_{x,left} \\ \Delta F_{x2} = 0 \\ \Delta F_{x4} = 0 \end{cases}$$

$$with\, \Delta F_{x,left} = \frac{M_{z,des}}{t_w / 2}$$

$$M_{z,des} < 0$$

$$\Rightarrow \begin{cases} \Delta F_{x1} = 0 \\ \Delta F_{x3} = 0 \\ \Delta F_{x2} = \dfrac{\left|\Delta F_{x2,\max}\right|}{\left|\Delta F_{x2,\max} + \Delta F_{x4,\max}\right|} \Delta F_{x,right} \\ \Delta F_{x4} = \dfrac{\left|\Delta F_{x4,\max}\right|}{\left|\Delta F_{x2,\max} + \Delta F_{x4,\max}\right|} \Delta F_{x,right} \end{cases}$$

$$with\, \Delta F_{x,right} = \frac{M_{z,des}}{t_w / 2}$$

where,

$$\Delta F_{x1,\max} = F_{x1} - \sqrt{(\mu F_{z1})^2 - (F_{y1l})^2}$$

$$\Delta F_{x3,\max} = -F_{x3} - \sqrt{(\mu F_{z3})^2 - (F_{y3})^2}$$

$$\Delta F_{x2,\max} = F_{x2} - \sqrt{(\mu F_{z2})^2 - (F_{y2})^2}$$

$$\Delta F_{x4,\max} = -F_{x4} - \sqrt{(\mu F_{z4})^2 - (F_{y4})^2} \qquad (25)$$

Chapter 4. Simulation Results

In order to analyze the effect of stochastic robust LQR, double lane change case described in Figure 4.1 and decreasing radius curve depicted in Figure 4.2 were used as scenarios considering [4]. Vehicle's speed was 70kph and control performance was compared between nominal case and uncertain case for double lane change scenario. Nominal case is composed of parameters with nominal states. Uncertain case is comprised of mass with the value of 500kg larger than nominal value, tire-road coefficient of 0.6, l_f which is 0.3 m larger than its nominal value.

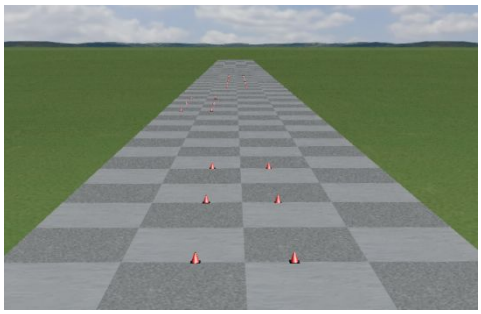

(a) The Whole View of the Scenario

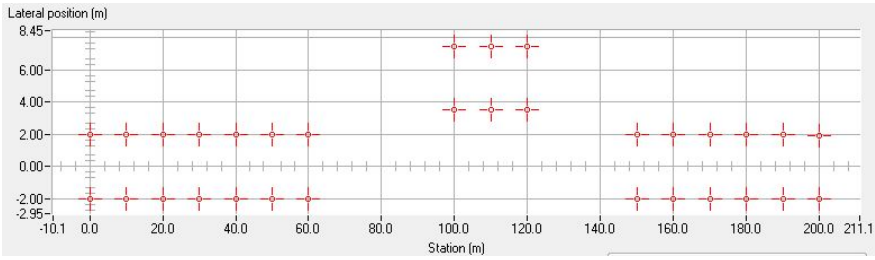

(b) Road Profile

Figure 4.1 Double Lane Change Scenario

(a) The Whole View of the Scenario

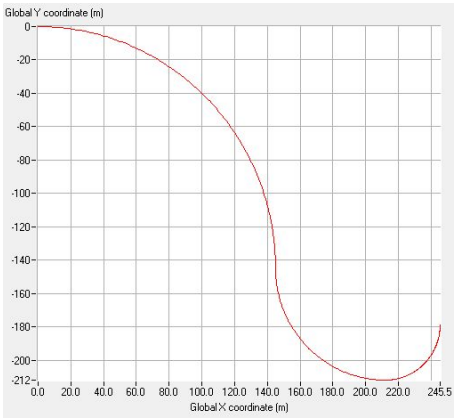

(b) Road Profile

Figure 4.2 Decreasing Radius Curve Scenario

Control performance was analyzed with yaw rate tracking error. To check the robust effect, stochastic robust LQR was compared with conventional LQR. In case of conventional LQR, their control parameters are determined randomly but to guarantee stability of the system. In order to check the effect of robust control for double lane change, vehicle trajectory, yaw rate error, steering angle with uncertain state were analyzed, and they are described in Figure 4.3

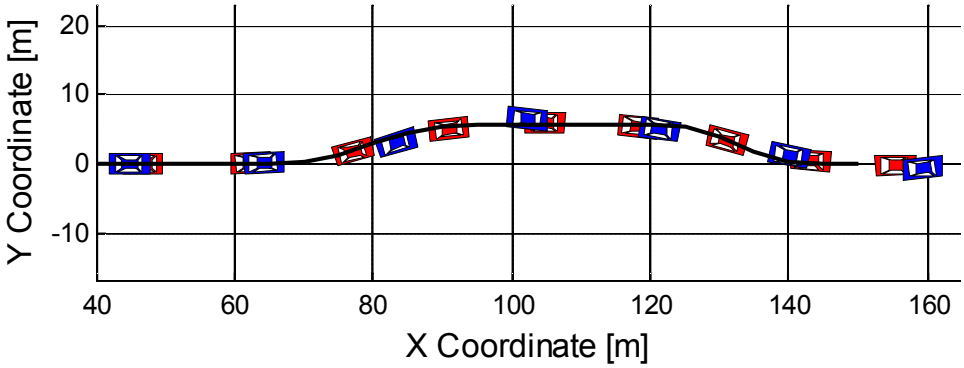

(a) Vehicle Trajectory(red : robust / blue : conventional)

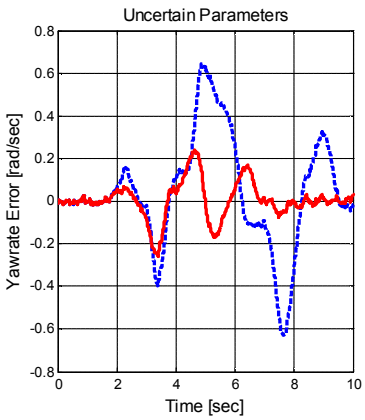

(b) Yaw Rate Error

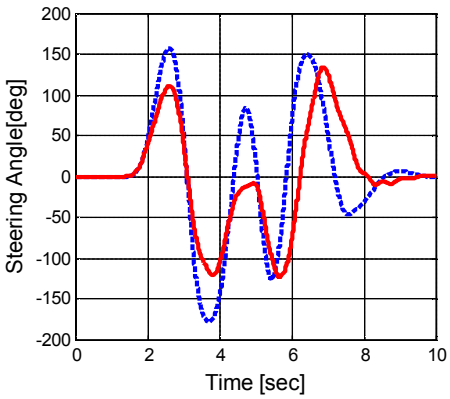

(c) Steering Angle

Figure 4.3 Results with Uncertain State(Double Lane Change)

For the case of decreasing radius curve, vehicle trajectory, yaw rate error, steering angle with uncertain state were analyzed, and they are described in Figure 4.4 Test velocity was 90kph.

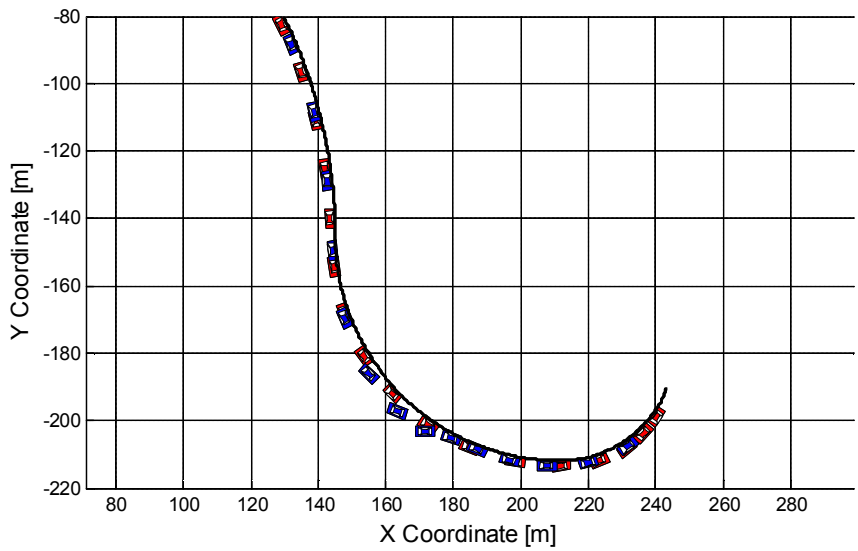

(a) Vehicle Trajectory(red : robust / blue : conventional)

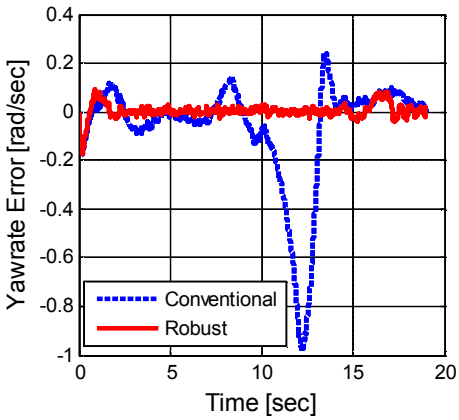

(b) Yaw Rate Error

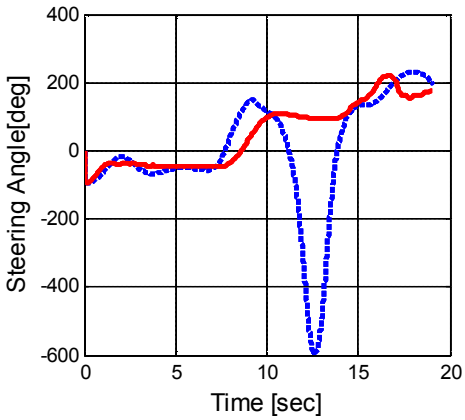

(c) Steering Angle

Figure 4.4 Results with Uncertain State(Decreasing Radius Curve)

To evaluate the robust performance, yaw rate errors were analyzed with the cases between one that the vehicle have nominal parameters and the other which is comprised of uncertain parameters. Their results are plotted in Figure 4.5

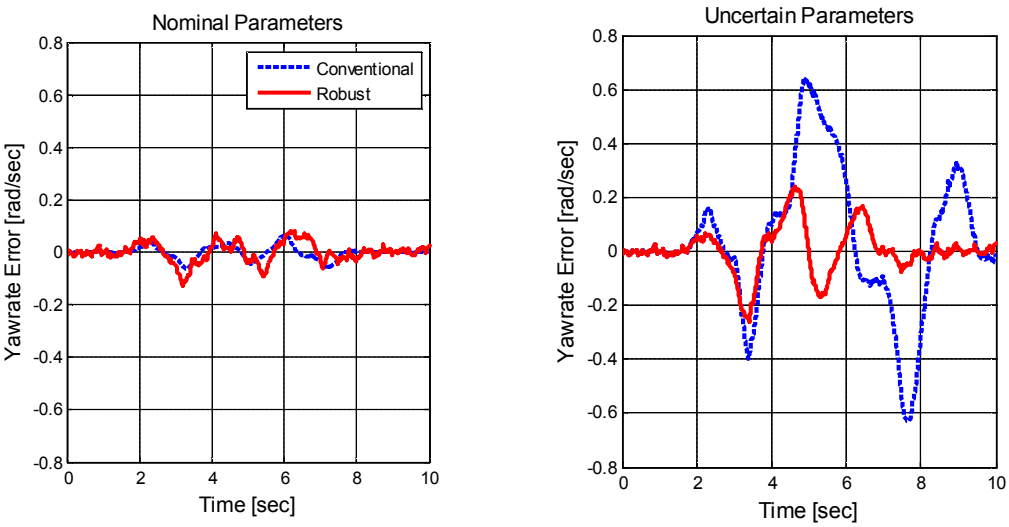

(a) Nominal Parameters (b) Uncertain Parameters

Figure 4.5 Robust Performance(Double Lane Change)

Robust performance can be analyzed with respect to a single parameter. For example, with respect to changes of l_f, yaw rate RMSE is plotted in Figure 4.6

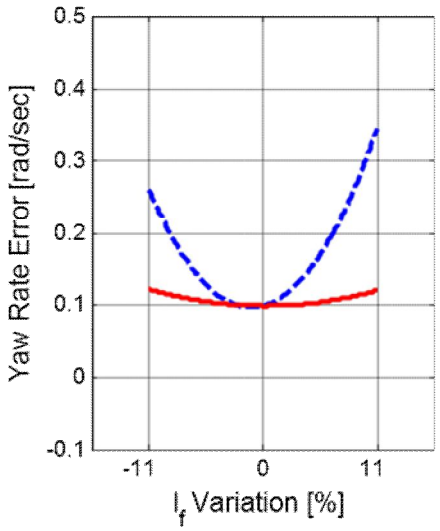

Figure 4.6 Yaw Rate RMSE w.r.t. l_f

Chapter 5. Summary/Conclusions

Robust control that remedies the uncertainty of commercial vehicles was developed in this paper. Even though control performances with nominal state are similar between conventional LQR and stochastic robust LQR, with uncertain state, there is a large gap in control performances between them. In the process of finding design parameters for conventional LQR, it is tedious and difficult to find suitable design parameters. However, taking stochastic root locus and sensitivity dynamics into account, optimal point that deals with parametric uncertainty and guarantees stability, robustness can be determined. Moreover, slight changes in yaw motion or roll angle can endanger commercial vehicles. Therefore, robust control is much more needed for commercial vehicles than for passenger vehicles.

Bibliography

[1] National Highway Traffic Safety Administration, “Proposed FMVSS No. 126 - Electronic Stability Control Systems”, August 2006

[2] National Center for Statistics and Analysis, National Highway Traffic Safety Administration, Traffic Safety Facts - Large Heavy vehicles, DOT HS 811 158, 2009.

[3] National Highway Traffic Safety Administration, “FMVSS No. 136 - Electronic Stability Control Systems on Heavy Vehicles”, May 2012

[4] National Highway Traffic Safety Administration, “Heavy Truck ESC Effectiveness Study Using NADS – Final Report”, November 2009

[5] Jangyeol Yoon, Wanki Cho, Bongyeong Koo, Kyongsu Yi, “Unified Chassis Control for Rollover Prevention and Lateral Stability”, IEEE TRANSACTIONS ON VEHICULAR TECHNOLOGY, VOL. 58, NO. 2, FEBRUARY 2009

[6] B. L. Boada, M. J. L. Boada, V. Diaz, “Fuzzy-logic applied to yaw moment control for vehicle stability”, Vehicle System Dynamics, Vol. 43, No. 10, October 2005, 753-770

[7] Sinan Oncu, Sertac Karaman, Levent Guvenc, S.Server Ersolmaz, E.Serdar Ozturk, Emre Cetin, Mustafa Sinal, “Robust Yaw Stability Controller Design for a Light Commercial Vehicle Using a Hardware in the Loop Steering Test Rig”, 2007 IEEE Intelligent Vehicles Symposium, Istanbul, Turkey, 2007.

[8] Chien Chen, Masayoshi Tomizuka, “Lateral Control of Commercial Heavy Vehicles”, Vehicle System Dynamics, Vol 33, No.6, 391-420

[9] Tankut Acarman, Umit Ozguner, “Rollover preventin for heavy trucks using frequency shaped sliding mode control”, Vehicle System Dynamics, Vol 44, No.10, 737-762

[10] Robert F. Stengel, Laura R. Ray, “Stochastic Robustness of Linear Time-Invariant Control Systems”, IEEE TRANSACTIONS ON AUTOMATIC CONTROL, VOL. 36, NO. I, JANUARY 1991

[11] Qian Wang, Robert F. Stengel, “Robust Control of Nonlinear Systems with Parametric Uncertainty”, Proceedings of the 37th IEEE Conference on Decision & Control,Tampa, Florida USA December 1998

[12] Rajesh Rajamani, “Vehicle Dynamics and Control”, 2007 Springer

[13] E. Esmailzadeh, A Goodarzi, G.R. Vossoughi, “Optimal yaw moment control law for improved vehicle handling”, Mechatronics, Volume 13, Issue 7, September 2003, Pages 659–675

[14] Anthony J. Calise, Edward V. Byrns Jr., “Parameter Sensitivity Reduction in Fixed-Order Dynamic Compensation”, Journal of Guidance, Control, and Dynamics, Vol. 15, No. 2, March-April 1992

[15] Daniel D. Moerder, Anthony J. Calise, “Convergence of a Numerical Algorithm for Calculating Optimal Output Feedback Gains”, IEEE TRANSACTIONS ON AUTOMATIC CONTROL, VOL. AC-30, NO. 9, SEPTEMBER 1985

초 록

이 논문은 상용차량의 요 안정성 제어에 대한 내용을 다루고 있다. 상용차량에 관해서는 그들의 고유한 특성들 – 무게중심, 차량의 너비, 하중 분포 – 이 그들을 요 불안정성에 대해 취약하게 만든다. 상용차량의 경우 승용차량에 비해 그들의 작업 환경 등으로 인해 차량 변수들의 변화가 크다. 차량의 질량, 코너링 강성, 무게중심 등의 변수들의 변화는 차량의 근궤적의 변화를 가져온다. 이에 대해 강건한 성능을 보장하기 위해 확률적 근 궤적과 민감도 분석을 고려한 강건 제어기가 사용되었다. 시뮬레이션 해석이 이 제안된 제어기를 통해 수행되었다. 시뮬레이션을 통해 차량 변수들의 변화에 대한 강건한 성능이 보장됨을 확인할 수 있었다.

주요어 : 차체 자세 제어 장치, 요 안정성 제어, 확률적 근 궤적, 민감도 분석, 선형제곱조정기

학 번 : 2012 - 20666